

CHANDRA Observations of X-Ray Jet Structure on kpc to Mpc Scales

D. A. Schwartz^{a *}, H. L. Marshall^b, B. P. Miller^b, D. M. Worrall^c, M. Birkinshaw^c,
J. E. J. Lovell^d, D. L. Jauncey^d, E. S. Perlman^e, D. W. Murphy^f, R. A. Preston^f

^aHarvard-Smithsonian Center for Astrophysics
60 Garden St., Cambridge, MA 02138, USA

^bMassachusetts Institute of Technology
NE80-6031, Cambridge, MA 02139, USA

^cUniversity of Bristol, Dept. of Physics
Tyndall Ave., Bristol BS8 1TL, United Kingdom

^dCSIRO Australia Telescope National Facility
P.O. Box 76, Epping, NSW 2121, Australia

^eUniversity of Maryland, Baltimore Campus
Physics Department, 1000 Hilltop Dr., Baltimore, MD 21250, USA

^fJet Propulsion Laboratory
4800 Oak Grove Dr., Pasadena, CA 91109, USA

With its exquisite spatial resolution of better than 0.5 arcsecond, the *Chandra* observatory is uniquely capable of resolving and studying the spatial structure of extragalactic X-ray jets on scales of a few to a few hundred kilo-parsec. Our analyses of four recent Chandra images of quasar jets interpret the X-ray emission as inverse Compton scattering of high energy electrons on the cosmic microwave background. We infer that these jets are in bulk relativistic motion, carrying kinetic powers upwards of 10^{46} ergs s^{-1} to distances of hundreds of kpc, with very high efficiency.

1. INTRODUCTION

From our complete snapshot sample of quasar jets [1,2], we discuss here the four objects with the best statistical significance. These four powerful radio quasars span a redshift range from 0.591 to 1.455, and illustrate a range of morphological and physical effects.

We will compute source sizes and luminosities for a flat, accelerating cosmology, with $H_0=65$ km s^{-1} Mpc $^{-1}$, $\Omega_m = 0.3$, and $\Omega_\Lambda = 0.7$, and use the formulas given by [3]. For these jets, an $H_0=50$, $q_0 = 0.5$ cosmology changes lengths by $\leq 8\%$ and luminosities by $\leq 16\%$.

*This work was supported in part by NASA contract NAS8-39073 to the *Chandra* X-ray Center, NASA grant GO2-3151C to SAO, and SAO SV1-61010 to MIT. E.S.P. acknowledges support from NASA LTSA grant NAG5-9997.

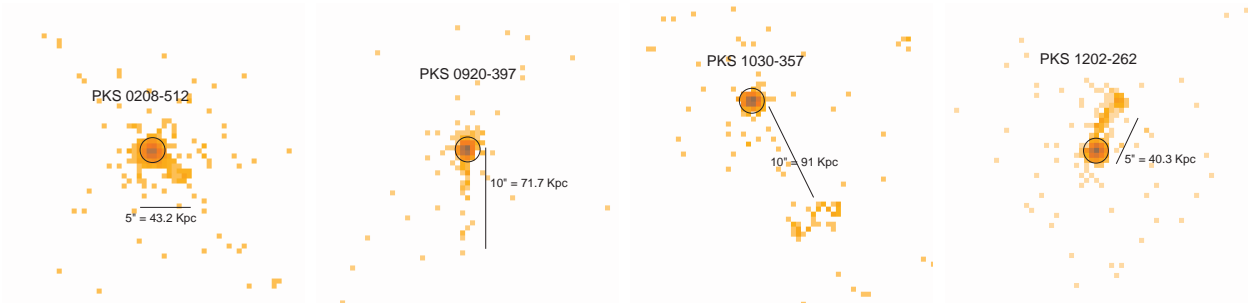


Figure 1. X-ray counts in 0.5 to 7 keV range, binned in $0''.49$ ACIS pixels.

2. MORPHOLOGIES

The jets in these four objects display a variety of X-ray morphology (Figure 1). The forms include the following: Straight jets from core: PKS 0208-512, PKS 0920-397; curved jets and straight jets which do not project to core: PKS 1202-262, (like PKS 0637-752 [4]); gaps between core and jet: PKS 1030-357(?), (like 3C 273 [5], and PKS 0637-752); jet emerges from core, disappears, resumes: PKS 0920-397, PKS 1030-357(?), (like Pic A [6]); X-ray to radio ratio roughly constant: PKS 1202-262, (like PKS 0637-752); X-ray decreases away from core, radio increases: PKS 0920-397, (like 3C 273); X-rays disappear when radio bends by large angle: PKS 0208-512, PKS 1202-262, (like PKS 0637-752), *exception*: PKS 1030-357. We suggest that all these features are manifestations of small angular changes in jets which are beamed toward our line of sight.

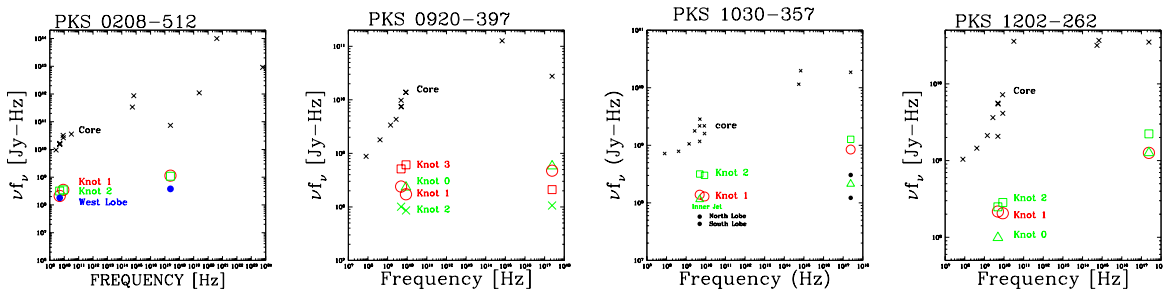


Figure 2. SED for the quasar cores, and for each subregion of the four jets. (Knot numbers increase away from the core.)

3. EMISSION MECHANISMS

We divide the jets into distinct regions, to compare the changing X-ray and radio structure. For each source we extract both the X-ray and radio flux densities, and construct the broad-band Spectral Energy Distributions (Figure 2). (We may have $\sim 20\%$ inaccuracies

as we have not smoothed the radio and X-ray data to correspond to the same angular resolution.) The jet radiative power is typically dominated by the X-ray emission. Note the significant detection of X-rays from radio lobes in PKS 0208-512 and PKS 1030-357.

For the gamma-ray blazar PKS 0208-512 we have measured [7] an upper limit to the optical emission of the jet which does not allow the X-rays to be a simple extrapolation of the radio synchrotron emission. For some knots in the other sources, our two point radio spectral index also argues against such extrapolation. We will assume that the X-ray emission from all the knots arises from inverse Compton (IC) scattering by the same power law population of electrons which emits the radio synchrotron radiation.

The ratio of synchrotron to Compton flux densities at any frequency is just the ratio of energy density of the magnetic field to the energy density of the target photons [8]. In applying that formula to the powerful X-ray jets, one typically cannot find a credible source of target photons if one also assumes that the magnetic field, B , and relativistic electrons are within an order of magnitude of their equipartition values (e.g. [4]). This dilemma was resolved by [9,10] by exploiting the Γ^2 enhancement of the apparent CMB density in a frame moving with bulk relativistic velocity with respect to the isotropic CMB frame [11].

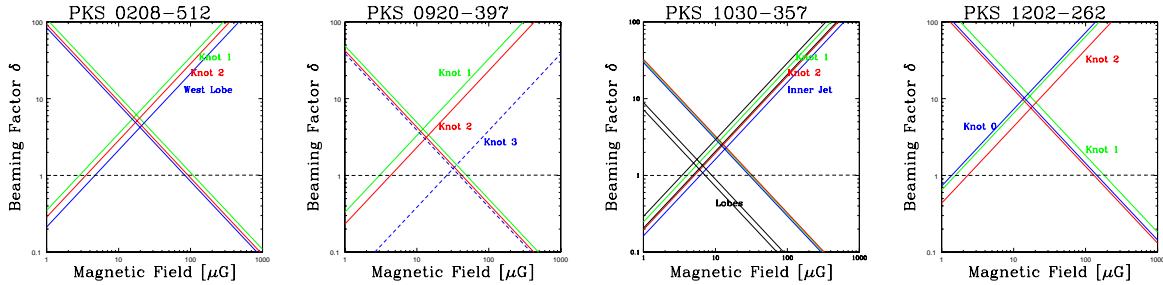


Figure 3. The equipartition conditions (lines decreasing with magnetic field) and the conditions for production of the X-rays by IC/CMB (lines increasing with magnetic field), intersect to give an estimate of the rest frame magnetic field and of the bulk relativistic beaming factor δ .

A jet in bulk relativistic motion at an angle θ to our line of sight is characterized by the beaming factor $\delta = (\Gamma(1 - \beta \cos \theta))^{-1} = (\Gamma(1 - \sqrt{1 - 1/\Gamma^2} \cos \theta))^{-1}$. We have independent equations from the equipartition condition, and from the condition that the electron population producing the synchrotron radio emission also produces the X-rays via inverse Compton scattering on the CMB. In Figure 3 the intersections of these relations for each feature of each of the four sources give solutions for the unknowns δ and B . We see a pattern of magnetic fields of order $10 \mu\text{G}$ and relativistic beaming factors 2 to 10 in the jets. There is a hint that the δ values decrease away from the cores; however, one needs to consider a factor of a few uncertainty in B , since exact equipartition of energy need not apply, and since the values we assume for the other parameters in the equipartition calculation are not well determined.

Table 1
Chandra Observations of X-Ray Jets

PKS Name ^a	z^a	L_x^b	Jet Fraction ^c	$\langle B \rangle$ [μG]	$\langle \delta \rangle$	θ_{max}	L^d	P_j^e	Radiative Efficiency ^f
0208-512	0.999	6.3	0.035	18	5.5	10.5	220	12	0.002
0920-397	0.591	0.74	0.062	13	3.6	16	230	1	0.005
1030-357	1.455	3.5	0.16	12	2.5	24	335	4.5	0.012
1202-262	0.789	1.78	0.14	15	10.6	5.4	470	5	0.005

^aNED, operated by JPL for NASA. ^bRest frame 2–10 keV luminosity of quasar core, in 10^{45} ergs s^{-1} . ^cX-ray flux ratio, jet to core. ^dMinimum length of X-ray jet, in kpc. ^eKinetic power of jet, 10^{46} erg s^{-1} . ^fRadiative power of jet, as a fraction of its kinetic power.

We take a mean value of the magnetic field and of the beaming factors to characterize the jet, as shown in Table 1. For any beaming factor δ , the maximum angle between the jet and our line of sight is $\theta_{max} = \cos^{-1}[(\delta - 1/\delta)/\sqrt{(\delta^2 - 1)}]$. From this maximum angle, and the measured projection of the jet on the sky, we can compute the minimum intrinsic length of each jet, as given in column 8. We estimate the kinetic power transported by the jet as $A\Gamma^2cU$, where A is the cross sectional area, Γ is assumed equal to δ , and U is the total energy density in the jet rest frame (cf. [12]). A minimum power (column 9) results for an electron/positron jet, as distinct from an electron/proton jet. These powers are typically larger than the bolometric luminosity of the quasar, (cf. Fig. 2). The low efficiency, column 10, with which these jets radiate their kinetic power is consistent with the ability to transport energy from the black hole core to distant radio lobes. Specifically in the case of PKS 0208-512, the power carried by the jet on scales of 100 kpc is shown to be comparable to the power in the pc scale jet as estimated by [13].

REFERENCES

1. H.L. Marshall, et al., *New Astronomy Review* (2003), this volume.
2. D.A. Schwartz, et al., *Active Galactic Nuclei*, (2003) in press
3. Pen, U-L. 1999, *Ap.J. Suppl.*, 120, 49
4. D.A. Schwartz et al., *Ap.J. (Lett)*, 540 (2000) L69.
5. H.L. Marshall, et al, *Ap.J.* 549 (2001) L167.
6. A.S. Wilson, A.J. Young, & P.L. Shopbell, *Ap.J.* 547 (2001) 740.
7. B.P. Miller, undergraduate thesis, M.I.T. (2002).
8. J.E. Felten and P.R. Morrison, *Ap.J.* 146 (1966) 686.
9. F. Tavecchio, et al., *Ap.J. (Lett)*, 544 (2000) L23.
10. A. Celotti, G. Ghisellini, & M. Chiaberge, *MNRAS*, 321 (2001) L1.
11. C.D. Dermer, & R. Schlickeiser, *ApJS*, 90 (1994) 945.
12. G. Ghisellini, & A. Celotti, *MNRAS*, 327 (2001) 743.
13. L. Maraschi, & F. Tavecchio, *astro-ph/0205252* (2002).